

Comparison of Controllers with Current Droop Capability for Series-connected Autonomous Distributed Modular Power Converter

Koki Yamanokuchi, Hiroki Watanabe, Jun-ichi Itoh
*Department of Electrical, Electronics, and Information Engineering,
Nagaoka University of Technology, NUT
Nagaoka, Japan*

koki_yamanokuchi@stn.nagaokaut.ac.jp, hwatanabe@vos.nagaokaut.ac.jp, itoh@vos.nagaokaut.ac.jp

Abstract— This paper reveals the performance of the feedback controller with the current droop control for autonomous distributed modular power conversion systems. The current droop control implemented to decouple the series-connected power modules causes the instability when a traditional PI controller is applied. This paper compares the closed-loop frequency response and root locus of the P, PI, IP, and PR controller when the current droop controller is applied. The experimental results of the system with 500 W per module clarify that the current droop control has almost no effect on the bandwidth of the current controller. The stability limit of PI control agreed with the analytical results with an error of 1.3%. Furthermore, the appropriately designed gain of the current droop control does not deteriorate the disturbance suppression characteristics of the current controller.

Keywords— *droop control, autonomous decentralized control, Universal smart power module, feed-forward compensation*

I. INTRODUCTION

In recent years, the Power Electronics Building Block (PEBB) concept have been widely considered owing to its high system reliability and high system extensibility [1]-[3]. The high scalability of the PEBB system realizes simplification of the main circuit design because the system rating can be flexibly changed by simply stacking modules. In addition, the system has high reliability due to its redundant design because it can continue to operate even when one module in the system fails. However, the system design of PEBB requires the input/output filter and the central controller design as the traditional power converter design [4]-[5]. Therefore, PEBBs are not sufficient in terms of building blocks for power converters.

On the other hand, a novel power conversion module which called the Universal Smart Power Module (USPM) have been proposed [6]. USPM integrates all power converter elements such as input/output filters and high-speed controllers in addition to the conventional PEBB. The USPM-based power conversion system consists of USPMs and a master controller to manage the overall operation of the system. The contribution of USPM is the excellent versatility and extensibility because the USPM-based system provides the easy implementation for the power electronics design. USPM has high versatility to build any power conversion system just by changing the combination, because it can work as a control current source or control

voltage source.

In USPM-based system, the control of each USPM interferes due to the unbalance of internal parameters because each controller does not operate concertedly to the other controller in USPMs even though USPM is stacked with modules similar to PEBB. Then, the parallel drive of voltage control type power converters has been considered in many conventional autonomous distributed power converters [7]-[9]. In particular, the droop control is suitable for the USPM-based systems adopting the autonomous decentralized control because it does not require communication among other controllers. The droop control in voltage, frequency and active/reactive power has been applied in parallel drive of the voltage source type power converters such as microgrid [10]-[12]. On the other hand, the current droop control for driving current control type power converters in series has not yet been fully investigated for its effects on the conventional current controllers [13]. In addition, the current droop control should be considered with the effect on the voltage disturbance feed-forward (FF) compensation.

In this paper, the Proportional (P), Proportional Resonance (PR), Proportional Integrated (PI), and Integrated Proportional (IP) current controller with the current droop control are evaluated to clarify the performance of the feedback control. In addition, the FF compensation has been demonstrated to have an important influence on the current droop control. The originality of this paper is that it analyzes the response and stability of the current droop control, which has not been evaluated before.

The configuration of this paper is as follows. Chapter 2 explains the system configuration of the single-phase AC-AC power conversion system with USPM. Chapter 3 explains the concept of the current droop control applied to the current controlled module. Chapter 4 presents the characteristics of the current controller by control gain and plant parameters using closed-loop frequency analysis and root locus results of the current controller with current droop control. In Chapter 5, the characteristics compared in Chapter 4 are demonstrated by experimental results in a system with 500 W per module.

II. SYSTEM CONFIGURATION OF UNIVERSAL SMART POWER MODULE (USPM) CONCEPT

Fig.1 shows the circuit configuration of the single-phase AC-AC converter with USPMs. The main circuit of this

This work was supported by Council for Science, Technology and Innovation (CSTI), Cross-ministerial Strategic Innovation Promotion Program (SIP), “Energy systems of an Internet of Energy (IoE) society” (Funding agency: JST).

system consists of three types of USPMs: current control type, voltage control type, and isolation type. The primary and secondary USPMs consist of the H-bridge converter, the harmonic filter, the detection circuit, the gate driver, and the high-speed controller. The primary side grid current is controlled by USPM of current control type and the secondary side load voltage is controlled by USPM of voltage control type. The isolated USPMs is connected between the DC links in the primary and secondary USPMs to prevent circuit shorts. In the single-phase AC-AC converter system, USPMs are connected as the Input-Series-Output-Parallel (ISOP) because this configuration is able to reduce the voltage and current rating of USPMs. Note that the number of series and parallel USPMs and the connection configuration can be flexibly changed according to the specifications.

This system uses wireless communication between the master controller and USPM. The wireless communication does not allow the communication of instantaneous values because the data is exchanged in tens to hundreds of milliseconds. Thus, USPM uses the RMS command value instead of the instantaneous command value. Therefore, the master controller handles USPM as an independently controlled voltage or current source. However, the current control of each USPM interferes with each other because each controller does not operate in coordination with the other controllers when delays or gain errors occur due to temperature drift or settling errors in current detection. As a result, USPM causes the control failure due to over-modulation and voltage unbalance of USPM.

III. CURRENT CONTROL WITH CURRENT DROOP CONTROL

Fig.2 shows the equivalent circuit of the current droop control for decoupling between current source modules connected in series. Where v_g is the grid voltage, Y_d is the current droop gain, and k is the number of modules connected in series. Note that each current source means the current source converter with the current control. Usually, the current value of each current source should be become same owing to the series connection. Actually, these current values have the unbalance due to the error caused by the setting time and delay of current detection. The current droop control behaves as the parallel-connected resistor in order to compensate the current error for stabilization of the current control. The control failure due to current control interference is prevented even because the difference of current divided by $i_{ac,x}$ and $Y_{d,x}$ is equal in each module when each current $i_{ac,x}$ is unbalanced. The droop characteristic of the real current is given by;

$$i_{ac} = -\frac{Y_d v_g}{k} + \frac{1}{k} \sum_{y=1}^k i_y \quad (1).$$

The current droop control is considered in the dual theory of voltage droop control used in microgrids and other applications. The difference from the voltage droop control is that the current droop control effects the current control which is the most inner loop. This is meaning that the control gain and small delays caused by the control have a significant impact on the stability.

Fig.3 shows the control block diagrams of current control in USPM. In the analysis of each current controller, the plant

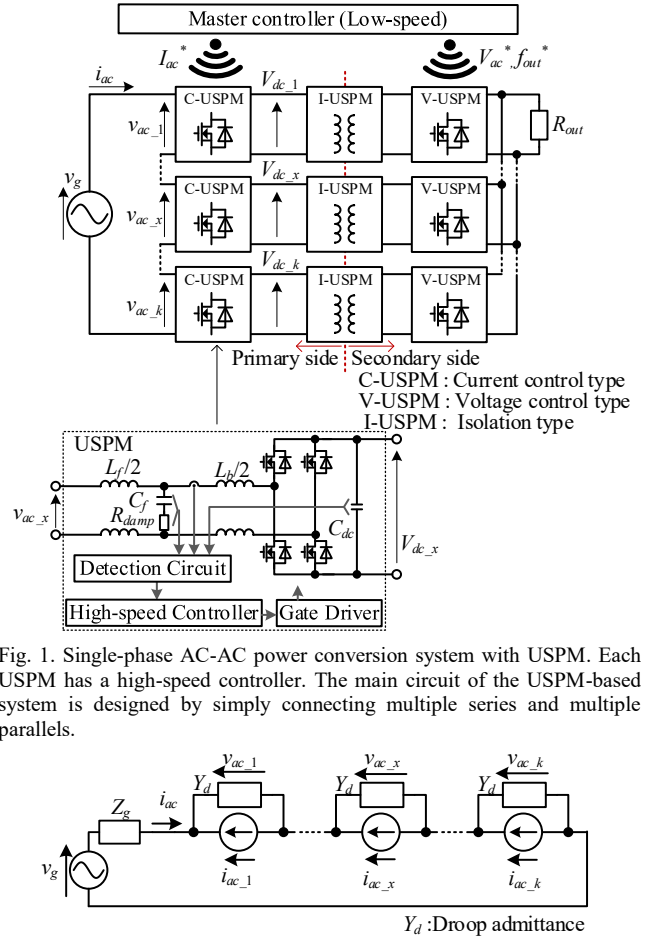


Fig. 1. Single-phase AC-AC power conversion system with USPM. Each USPM has a high-speed controller. The main circuit of the USPM-based system is designed by simply connecting multiple series and multiple parallels.

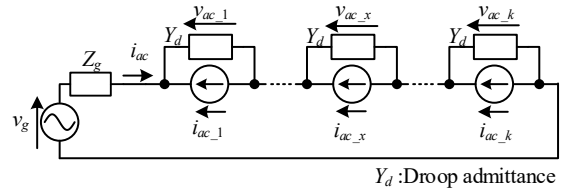


Fig. 2. Equivalent circuit of current droop control. The current droop control is implemented by inserting a virtual resistor in parallel to the controlled current source.

model is an L-filter configuration for simplicity. Furthermore, the delays due to USPM switching and detection are simulated by a first-order LPF. The current droop control is implemented by feeding back the inverter voltage command and the current droop gain Y_d to the current command. According to Fig. 3 (a)-(c), the recursive calculation appears in the controller loop within the loop in the controller. Therefore, the first-order delay is necessary, and it decays the transient characteristics of the system. On the other hand, the IP controller configuration in Fig. 3 (b) is able to eliminate the first-order delay.

IV. ANALYSIS RESULT OF EACH CONTROLLER

Table 1 shows the parameters for one module used in the analysis and experiments of this paper. In this paper, Y_d is varied from 0~1.0p.u. to check the change of characteristics with current droop gain. L_b is varied from 1 to 10% to check the change of characteristics with the plant model. The gain K_p and integration time T_i in the current controller are each designed to have a Butterworth arrangement of poles. The gain K_r of the PR control is designed to have the same disturbance suppression characteristics as the PI control at an operating frequency of 50 Hz.

A. Comparison of each controller

Fig.4 shows the closed-loop-frequency analysis result between the current command of i_{ac}^* and the actual current of i_L . According to Fig.4, the loop gain improves the

overshoot by suppressing the resonance when the droop gain

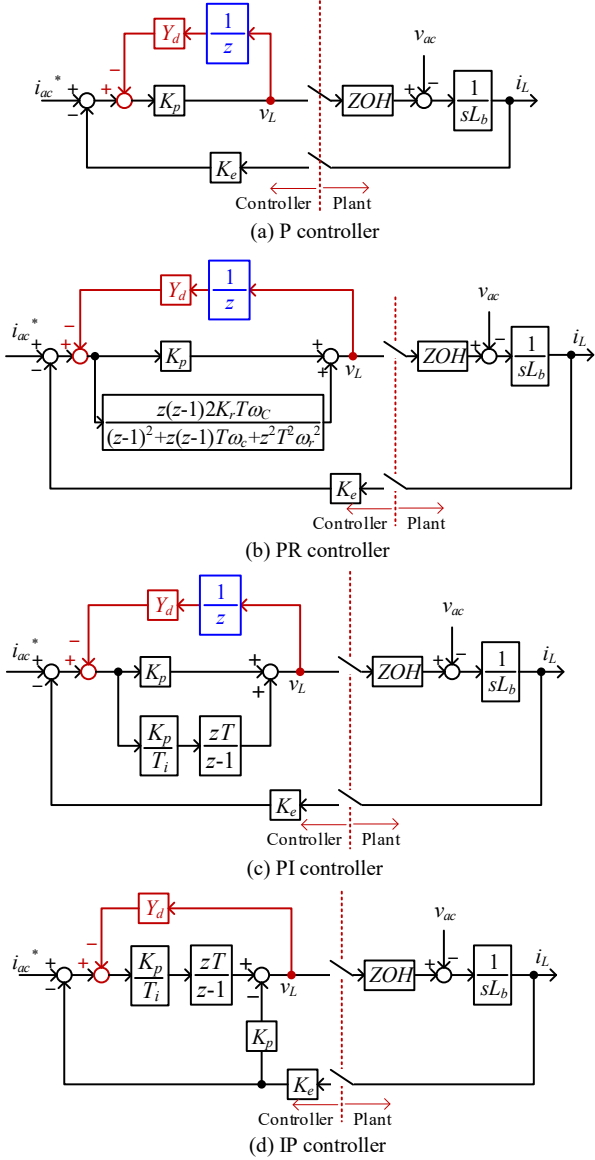


Fig. 3. Control block diagram of current control in USPM. The current droop control uses the command value by multiplying the output of the current controller by Y_d . The P, PR, and P controller requires a first-order delay while the IP controller does not.

Table 1. Analysis and experimental parameters.

Module Rated Power (1p.u.)	P	500 W
Module Rated AC Voltage (1p.u.)	V_{ac}	100 V
Rated AC Current (1p.u.)	I_{ac}	5 A
Rated admittance (1p.u.)	Y_n	0.05 S
Grid Frequency	f_g	50 Hz
DC link Voltage	V_{dc}	200 V
Sampling Frequency (=Switching Frequency)	f_{samp}	80 kHz
Proportional Gain of Current Control	K_p	1.444
Integral Time of Current Control	T_i	45.0 μ s
Resonance Gain of Current Control	K_r	100
Cutoff Freq. of Current Droop	f_{lpf}	5 kHz
Droop Admittance	Y_d	0~0.05 S(0~1.0p.u.)
Filter Inductor	L_f	650 μ H(%Z:1.02%)
Filter Capacitor	C_f	2.34 μ F(%Y:1.47%)
Boost Inductor	L_b	650 μ H(%Z:1.02%)
DC link Capacitor	C_{dc}	480 mF(H:19.2 ms)
Damping Resistor	R_{damp}	2 Ω

is increased. However, the PR, PI controller has unintended large gain and advanced phase around 40 kHz. This indicates that the system is moving in the direction of instability by increasing the droop gain. On the other hand, the droop gain does not almost influence the closed-loop characteristics when the IP controller is applied. Therefore, the outer loop control is designed without considering the effect of the current droop control even when the current droop control is applied. Therefore, IP controllers with high target value response are suitable for current controllers with the current

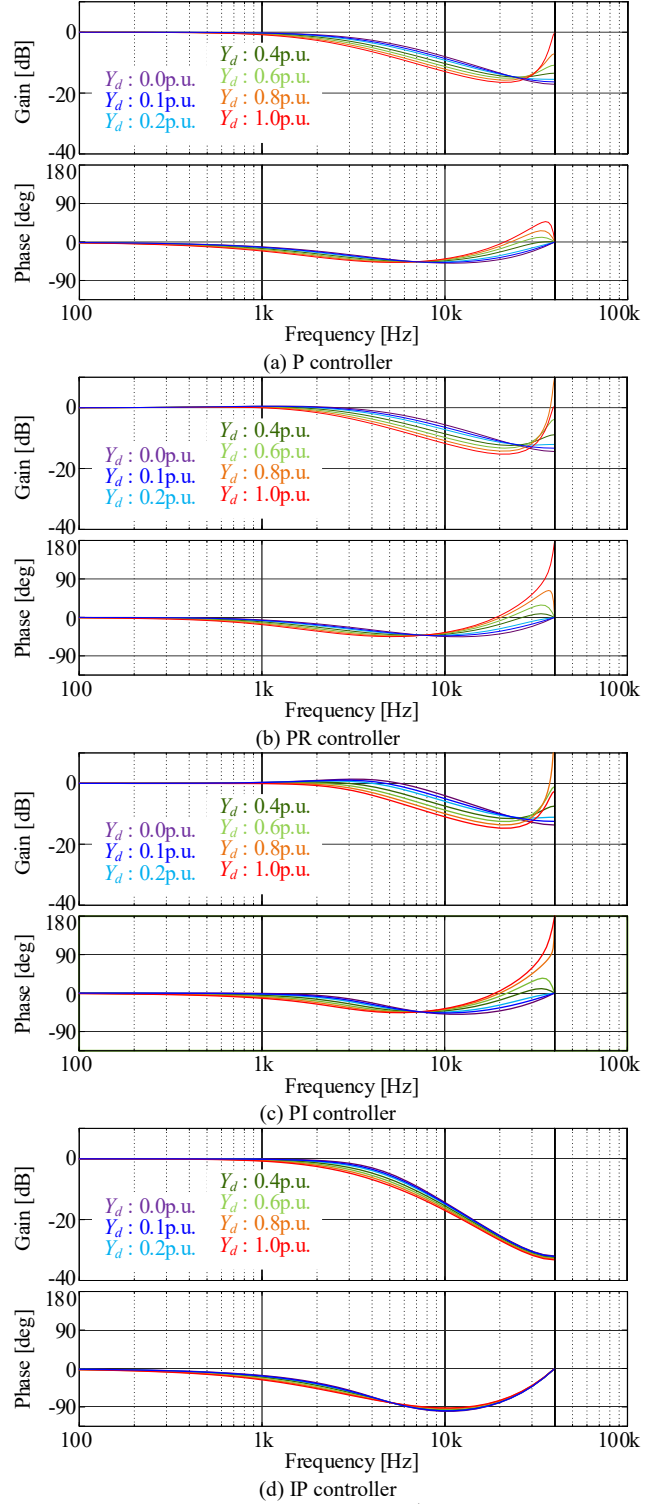


Fig. 4. Bode plots of transfer function from i_{ac}^* to i_L . Gain characteristics increase around 40kHz in the P, PR, PI control. IP control has almost no change in the gain and the phase characteristics.

droop control.

Fig.5 shows the closed-loop-frequency analysis result between the disturbance voltage of v_{ac} and the actual current of i_L . According to Fig. 5(a), the disturbance suppression characteristic of P control is more than 0 dB, which is very poor performance. According to Fig. 5(b), the resonant frequency component of PR control can achieve the same

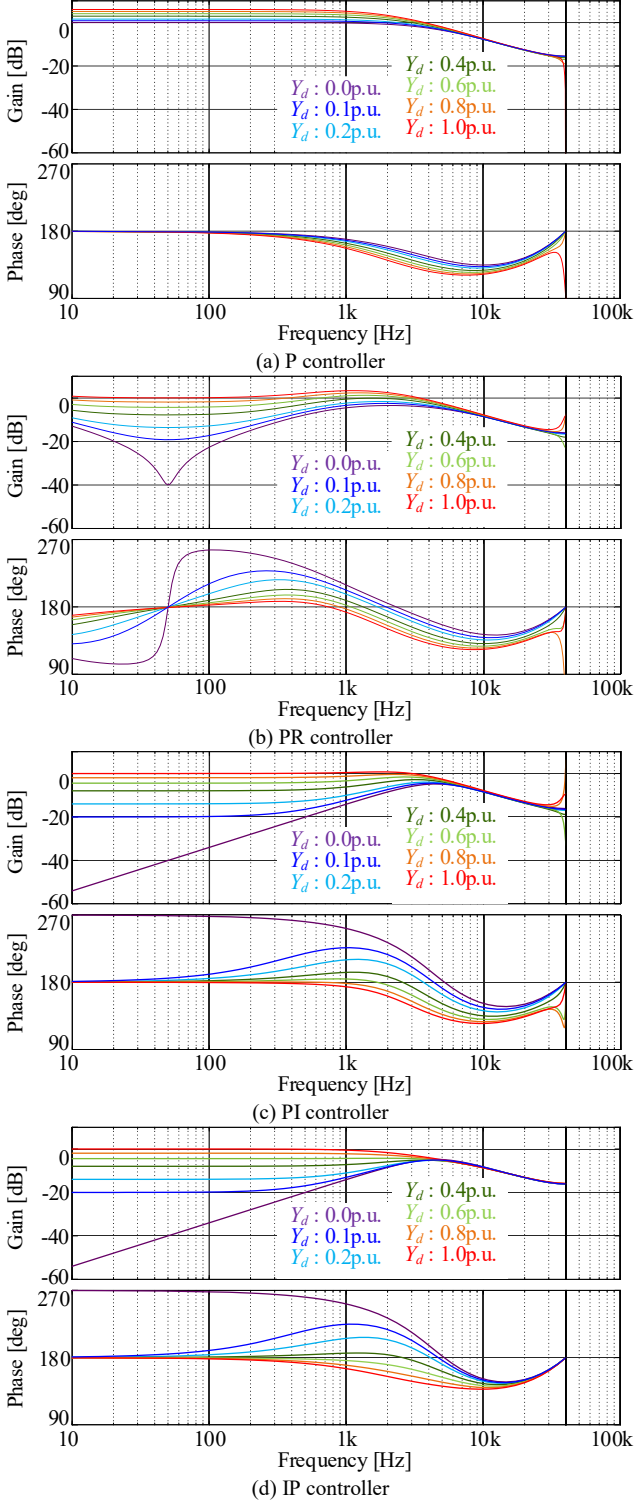


Fig. 5. Bode plots of transfer function from v_{ac} to i_L . The P and PR controllers have very worst characteristics in the frequency range without integration or differentiation. The characteristics of the low frequency range are the same for the PI and IP controllers. In the IP control, the disturbance response in the high frequency range near the peak is improved by current droop gain.

disturbance suppression characteristics as PI control and IP control, while USPM is not designed to operate at one determined frequency like grid-connected equipment. Thus, USPM is not suited for the controller of USPM because it requires a special design to match the operating frequency. According to Fig. 5(c) and 5(d), Two controllers have little difference because the current droop gain is dominant in the low frequency range below 1 kHz. The peak of the PI control increases as the current droop gain increases, while the peak of the IP control decreases. Therefore, the IP control is better able to suppress the disturbance near the peak of gain.

Fig.6 shows the root locus of the current control when varying the droop gain or boost inductor. Note that the boost inductor for varying the droop gain is 1%, and the droop gain for varying the boost inductor is 0.078 p.u. According to Fig.6 (a), the pole of the PR and PI controller moves to the outside of the unity circle when the droop gain is increased. The limit of Y_d for stable operation under this condition is 0.77p.u. In these controllers, the instability is avoided by changing the delay to LPF. However, the LPF requires to be designed for each controller because the gain characteristics change around the cutoff frequency. On the other hand, all poles are kept into the unity circle when the IP controller is applied. According to Fig.6 (b), the pole of the PI controller moves to the outside of the unity circle when the boost

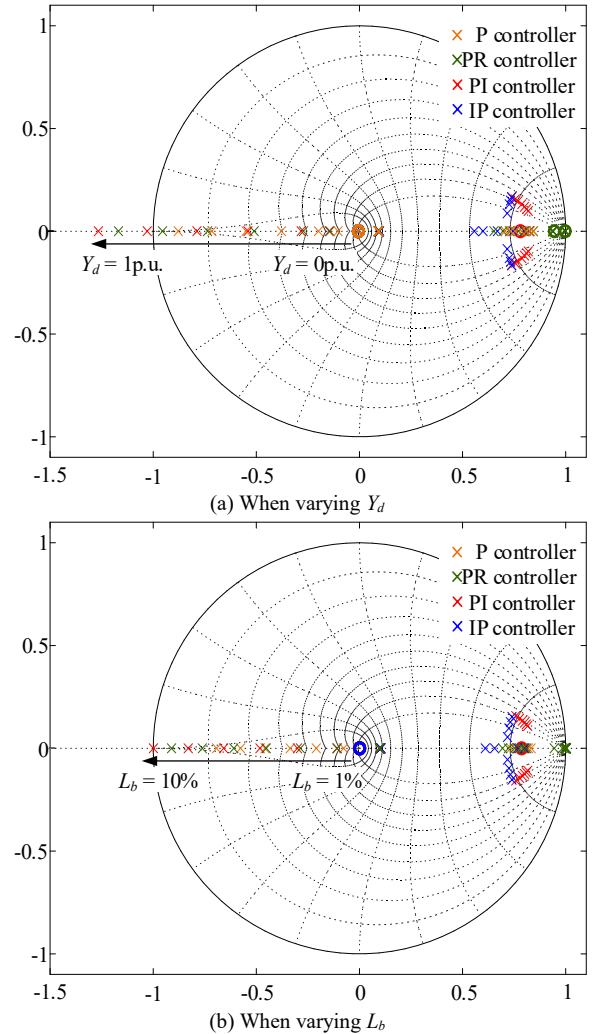


Fig. 6. Root locus of current control system when current droop gain is varied. The PR and PI control is unstable as the poles move outside the unity circle. The P and IP control is stable because the poles are within the unity circle.

inductor is increased. The limit of L_b for stable operation under this condition is 10%. The instability caused by droop control is suppressed by making L_b small. On the other hand, the control when L_b is small becomes difficult due to the impedance between the filter and the output side.

The features of each current controller that apply current droop control are as follows.

- P controller has the high stability limit. However, it is weak against the voltage disturbance.
- PR controller is highly resistant to the voltage disturbance of the specific frequency components. However, its stability limit is low. The PR controller reduces the versatility of USPM to operate at various frequencies.
- PI Controller is highly resistant to the voltage disturbance in the low frequency range. However, its stability limit is low.
- IP Controller is not only highly resistant to the voltage disturbance in the low frequency range, but also does not become unstable in the current droop control.

In summary, IP control is suitable for controllers applying the current droop control in terms of responsiveness and stability.

B. Comparison of each controller

Fig. 7 shows the block diagram of the IP current control system when the FF compensation is applied to the outside and inside of the current droop control loop. According to Fig. 7(a), the voltage feedback used for the current droop control is the estimated voltage of the inductor by applying the FF compensation outside the current droop control loop. According to Fig. 7(b), the voltage feedback used for the current droop control is the inverter voltage by applying the FF compensation inside the current droop control loop. Generally, the deterioration of the disturbance suppression characteristics on the low frequency side is suppressed by feed-forwarding the disturbance components to the current control output [14]. Nevertheless, the effect of disturbance feed-forward compensation is required to be considered because the current droop control adopts the inverter voltage as the control quantity.

Fig. 8 shows the disturbance suppression characteristics of the IP current control system when the FF compensation is applied outside and inside the current droop control loop. According to Fig. 8(a), the FF compensation of Fig. 7(a) provides the same characteristics as the disturbance suppression characteristics without the current droop control. However, this FF compensation does not provide the effect of droop control because the voltage feedback used for current droop control is the estimated voltage of the inductor. On the other hand, according to Fig. 8(b), the FF compensation in Fig. 7(b) gives a droop characteristic to the inverter voltage. Note that the disturbance suppression characteristics of this FF compensation deteriorate as in Fig. 5(d) because the disturbance suppression gain on the low frequency side is limited to Y_d as the droop gain increases. However, the required Y_d is less than 0.1 p.u. because the actual detection gain error is about $\pm 3\%$ at most. The disturbance suppression gain in the low frequency range sufficiently suppresses the disturbance voltage because it can

be obtained more than -20dB under the condition of Y_d is less than 0.1p.u. Therefore, the current droop control can suppress the disturbance by setting the droop gain appropriately without the FF compensation.

V. EXPERIMENTAL RESULTS

A rated load is connected to the primary in Fig. 1 to verify the validity of the analysis and discussion by the Bode and Nyquist diagrams. USPM is connected in series with two others.

Fig. 9 shows the target value response waveform when

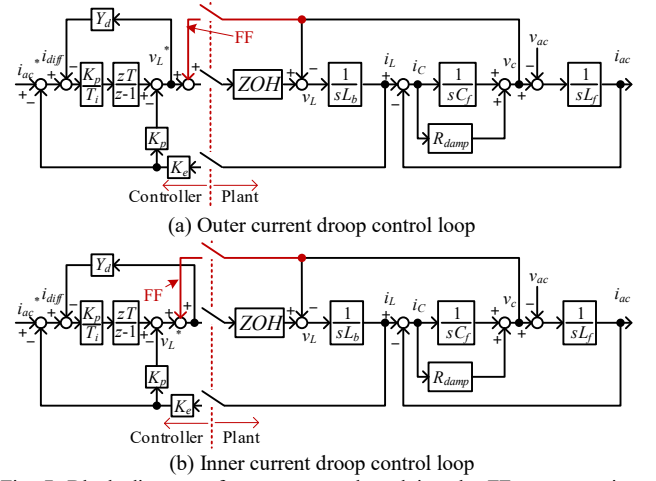


Fig. 7. Block diagram of current control applying the FF compensation. The current controller has the same disturbance suppression characteristics as the case without current droop control when the FF compensation is performed in Fig. 7(a). The current droop characteristics are the same as those without the FF compensation when the FF compensation is performed in Fig. 7(b).

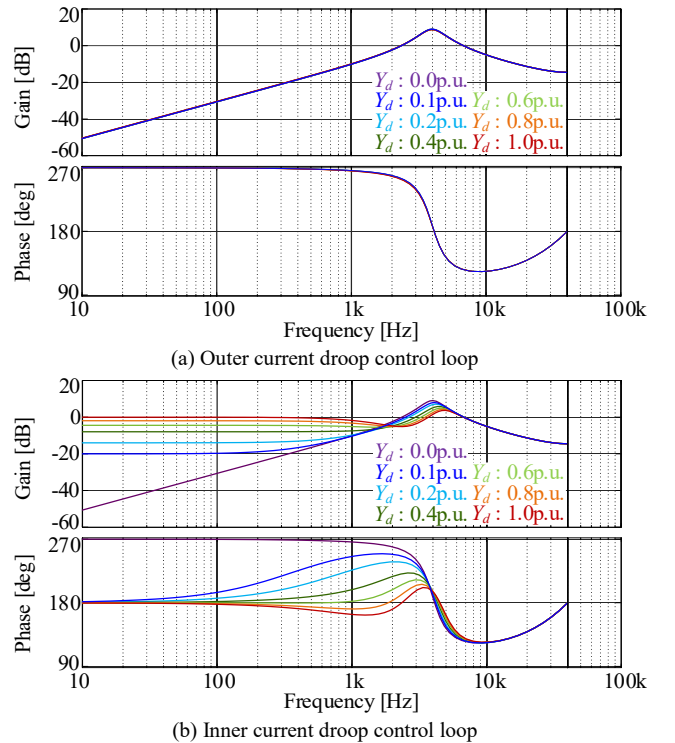
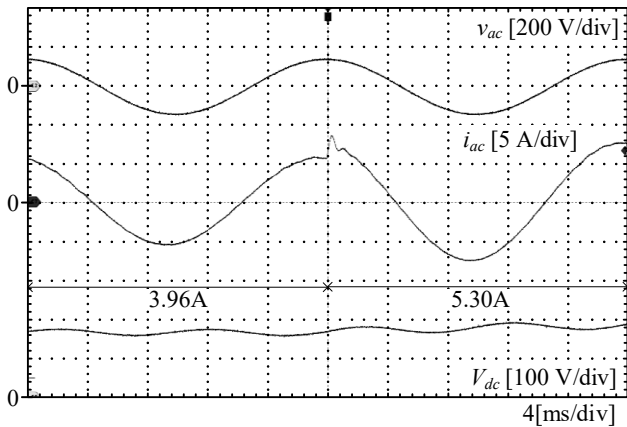


Fig. 8. Bode plots of transfer function from v_{ac} to i_L applying the FF compensation. Current controller provides same disturbance suppression characteristics as without current droop control when the FF compensation is performed in Fig. 8(a).

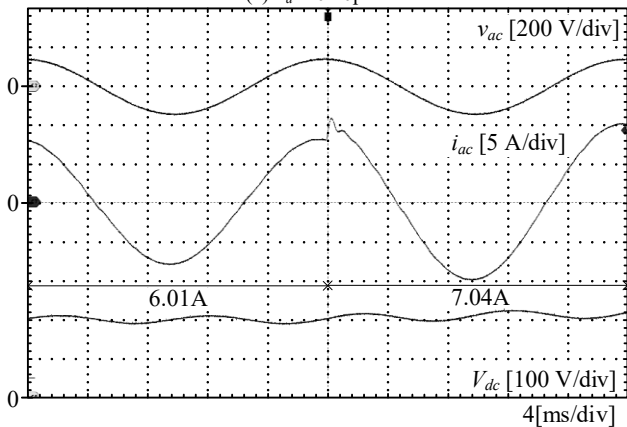
the command value is changed in steps from 1 p.u. to 0.7 p.u. at $Y_d = 0$ p.u., 0.2 p.u., and 0.5 p.u. According to Fig. 9, the response is consistent regardless of Y_d while the steady-state current value is different due to the droop characteristics of the current droop control. Therefore, the current droop control does not cause the bandwidth of the upper control system to be limited because it does not affect the command value responsiveness of the current control.

Fig. 10 shows the experimental results when the converter is started at each controller and Y_d . According to Fig. 10, the converter with PI controller works stably when Y_d is 0.76p.u. However, the operation is not keep due to overcurrent protection when Y_d changes to 0.77p.u. The stability limit of the experimental result matches the analysis well with an error of 1.3%. The cause of the instability Y_d is different from the stable analysis is the error of detection delay and inductance. On the other hand, the converter using the IP controller is stable even when Y_d is 1p.u.

Fig. 11 shows the input and output waveforms during the rated operation when the FF compensation in Fig. 7(a) is applied. Note that the current detection gain of USPM is intentionally unbalanced at +3% and -3% in order to check the effect of the current droop control. Thus, Y_d is set to 0.078 p.u. from the design equation in Ref. [13]. According to Fig. 11(a), the FF compensation in Fig. 7(a) has unbalanced AC and DC voltages due to the insufficient decoupling between modules. The RMS value of the AC current is not able to be decoupled because there is no current deviation due to the current droop control by being



(a) $Y_d = 0.10$ p.u.

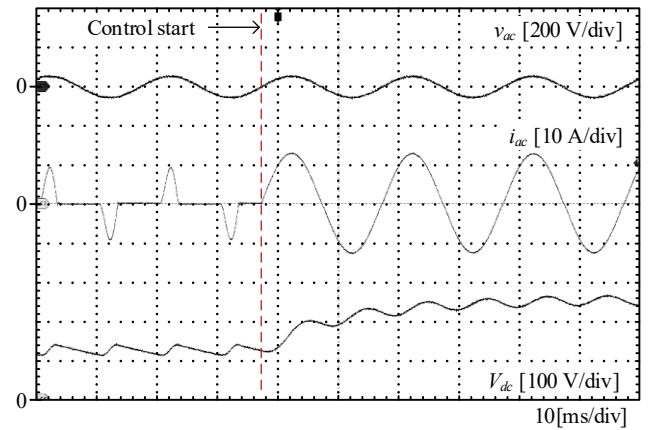


(b) $Y_d = 0.50$ p.u.

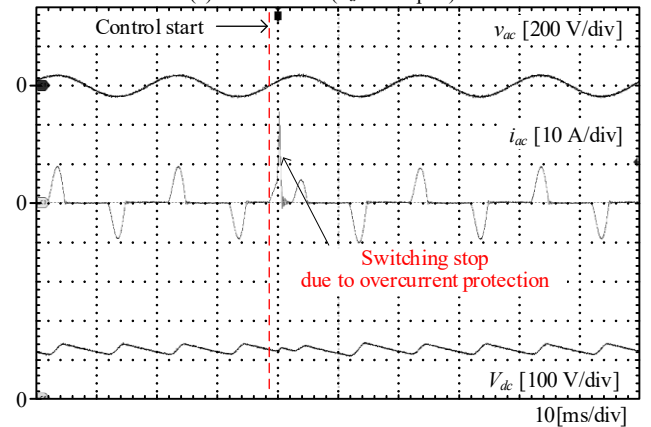
Fig. 9. Experimental waveform when the command value is varied. The transient response is almost unchanged although the RMS current value changes with the increase of Y_d .

lower than the command value of 1 p.u. On the other hand, according to Fig. 11(b) without the FF compensation, the voltage unbalance is improved in return for the increase in AC current.

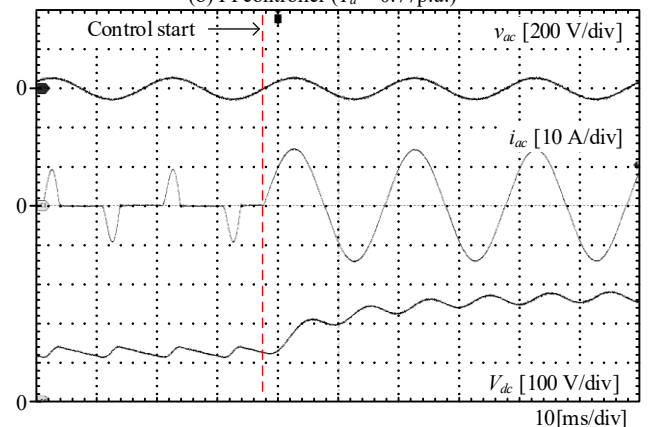
Fig. 12 shows the input and output waveforms at the time of grid voltage drop and recovery when the FF compensation in Fig. 7(b) is applied. Note that the grid voltage drops from 200 V to 100 V at the maximum positive voltage. Y_d is set to 0.078 p.u. as in Fig. 11. According to Fig. 12, the FF compensation in Fig. 7(b) does not completely remove the disturbance voltage of the system frequency component are 4.99 A and 5.20 A with and without the FF compensation. The reason is that the FF compensation in Fig. 7(b) deteriorates the disturbance suppression characteristics in the low frequency range as shown in Fig. 8(b). Note that the



(a) PI controller ($Y_d = 0.76$ p.u.)



(b) PI controller ($Y_d = 0.77$ p.u.)



(c) IP controller ($Y_d = 1.00$ p.u.)

Fig. 10. Startup operation waveform under each controller condition. The PI control stops working when Y_d increases due to overcurrent. IP control works stably even when Y_d is 1 p.u.

large surge current at the time of voltage fluctuation is not related to the droop control because it is a high frequency component. This large surge current is reduced by the proper design of the current regulator due to the small filter inductor.

VI. CONCLUSION AND FUTURE WORK

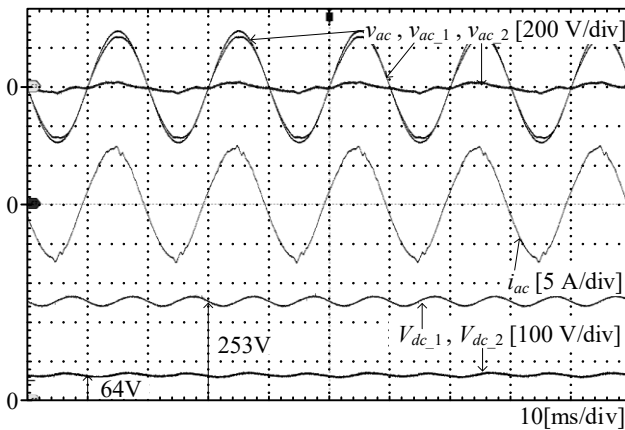
This paper evaluated the characteristics of the PI controller and the IP controller with the current droop control in order to improve the characteristics of the non-interference control applied to series-connected current source modules in a modular power conversion system with the autonomous decentralized control. In addition, this paper discusses the effect of the current droop control on the control system and the necessity of the FF compensation. The results of the frequency and stability analysis found that the current droop control did not affect the upper control band by not deteriorating the target value response performance. The current droop control minimized the deterioration of the disturbance suppression characteristics by setting Y_d appropriately. Furthermore, the results of the frequency analysis and stability analysis revealed that IP control is superior in both stability and responsiveness as a controller configuration to be implemented together with the current droop control. The IP controller is planned to consider control at saturation, which is a disadvantage in the future.

REFERENCES

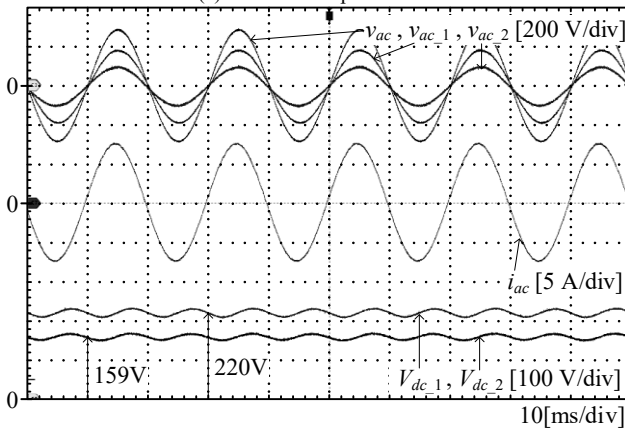
[1] W. Song and A. Q. Huang, "Fault-Tolerant Design and Control

Strategy for Cascaded H-Bridge Multilevel Converter-Based STATCOM," IEEE Trans. Industrial Electronics, vol. 57, no. 8, pp. 2700-2708, Aug. 2010.

- [2] A. R. Iyer, R. P. Kandula, R. Moghe, J. E. Hernandez, F. C. Lambert and D. Divan, "Validation of the Plug-and-Play AC/AC Power Electronics Building Block (AC-PEBB) for Medium-Voltage Grid Control Applications," IEEE Trans. Industry Applications, vol. 50, no. 5, pp. 3549-3557, Sept.-Oct. 2014.
- [3] E. Coulinge, S. Pittet and D. Dujic, "Design Optimization of Two-Quadrant High-Current Low-Voltage Power Supply," IEEE Trans. Power Electronics, vol. 35, no. 11, pp. 11602-11611, Nov. 2020.
- [4] Y. Jiao, S. Lu and F. C. Lee, "Switching Performance Optimization of a High Power High Frequency Three-Level Active Neutral Point Clamped Phase Leg," IEEE Trans. Power Electronics, vol. 29, no. 7, pp. 3255-3266, July 2014.
- [5] M. Guacci, D. Bortis, I. F. Kovačević-Badstübner, U. Grossner and J. W. Kolar, "Analysis and design of a 1200 V All-SiC planar interconnection power module for next generation more electrical aircraft power electronic building blocks," CPSS Trans. Power Electronics and Applications, vol. 2, no. 4, pp. 320-330, Dec. 2017.
- [6] K. Yamanokuchi, H. Watanabe and J. -I. Itoh, "Universal Smart Power Module Concept with High-speed Controller for Simplification of Power Conversion System Design," 2021 IEEE 12th Energy Conversion Congress & Exposition - Asia (ECCE-Asia), 2021, pp. 2484-2489.
- [7] Tsai-Fu Wu, Yu-Kai Chen and Yong-Heh Huang, "3C strategy for inverters in parallel operation achieving an equal current distribution," IEEE Trans. Industrial Electronics, vol. 47, no. 2, pp. 273-281, Apr. 2000.
- [8] D. Li and C. N. Man Ho, "A Delay-Tolerable Master-Slave Current-Sharing Control Scheme for Parallel-Operated Interfacing Inverters With Low-Bandwidth Communication," IEEE Trans. Industry Applications, vol. 56, no. 2, pp. 1575-1586, Mar.-Apr. 2020.
- [9] A. Micallef, M. Apap, C. Spiteri-Staines, J. M. Guerrero and J. C.

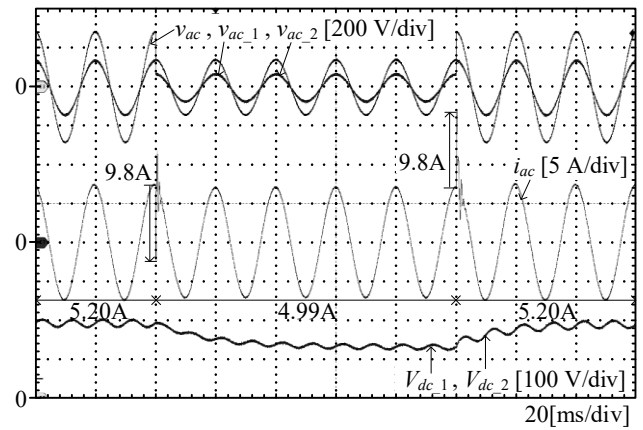


(a) With FF compensation

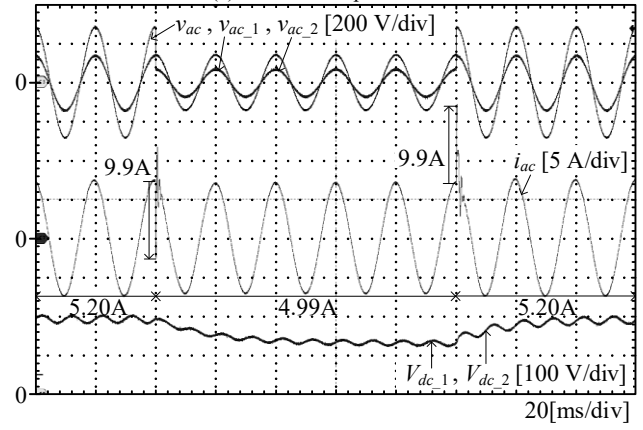


(b) Without FF compensation

Fig. 11. Effect of the FF compensation outer current droop control loop (Fig. 7 (a)). The voltage is unbalanced due to the interference of the current controller, although the current value follows the command value by the FF compensation.



(a) With FF compensation



(b) Without FF compensation

Fig. 12. Effect of the FF compensation inner current droop control loop (Fig. 7 (b)). The RMS current value with the FF compensation does not change compared to that without the FF compensation. The current deviation of 5% at the rated voltage indicates that the disturbance is sufficiently suppressed.

- Vasquez, "Reactive Power Sharing and Voltage Harmonic Distortion Compensation of Droop Controlled Single Phase Islanded Microgrids," *IEEE Transactions on Smart Grid*, vol. 5, no. 3, pp. 1149-1158, May 2014.
- [10] K. Rouzbehi, A. Miranian, J. I. Candela, A. Luna and P. Rodriguez, "A Generalized Voltage Droop Strategy for Control of Multiterminal DC Grids," *IEEE Trans. Industry Applications*, vol. 51, no. 1, pp. 607-618, Jan.-Feb. 2015.
- [11] G. Xu, D. Sha and X. Liao, "Decentralized Inverse-Droop Control for Input-Series-Output-Parallel DC-DC Converters," *IEEE Trans. Power Electronics*, vol. 30, no. 9, pp. 4621-4625, Sept. 2015.
- [12] M. Hamzeh, H. Karimi and H. Mokhtari, "A New Control Strategy for a Multi-Bus MV Microgrid Under Unbalanced Conditions," *IEEE Trans. Power Systems*, vol. 27, no. 4, pp. 2225-2232, Nov. 2012.
- [13] K. Yamanokuchi, H. Watanabe and J. Itoh, "Droop-based Current Control Method in Autonomous Distributed Modular Power Conversion System," 2021 IEEE Applied Power Electronics Conference and Exposition (APEC), 2021, pp. 660-667.
- [14] J. Ge, Z. Zhao, L. Yuan and T. Lu, "Energy Feed-Forward and Direct Feed-Forward Control for Solid-State Transformer," *IEEE Trans. Power Electronics*, vol. 30, no. 8, pp. 4042-4047, Aug. 2015.